Macrocyclic Hairpin Mimetics of the Cationic Antimicrobial Peptide Protegrin I: A New Family of Broad-Spectrum Antibiotics

Sasalu C. Shankaramma,[a] Zafiria Athanassiou,[a] Oliver Zerbe,[b] Kerstin Moehle,[a] Carole Mouton,[c] Francesca Bernardini,[c] Jan W. Vrijbloed,[a] Daniel Obrecht,[c] and John A. Robinson*[a]

The problems associated with increasing antibiotic resistance have stimulated great interest in newly discovered families of naturally occurring cationic antimicrobial peptides. These include protegrin, tachyplesin, and RTD-1, which adopt β-hairpin-like structures. We report here an approach to novel peptidomimetics based on these natural products. The mimetics were designed by transplanting the cationic and hydrophobic residues onto a β-hairpin-inducing template, either a D-Pro-L-Pro dipeptide or a xanthene derivative. The mimetics have good antimicrobial activity against Gram-positive and Gram-negative bacteria (minimal inhibitory concentration $\approx 6-25\ \mu g\,mL^{-1}$). Analogues with improved selectivity for microbial rather than red blood cells (1% hemolysis at $100\ \mu g\,mL^{-1}$) were identified from a small library prepared by parallel synthesis. Thus, it is possible to separate the antimicrobial and hemolytic activities in this class of mimetics. NMR studies on one mimetic revealed a largely unordered structure in water, but a transition to a regular β-hairpin backbone conformation in the presence of dodecylphosphocholine micelles. This family of mimetics may provide a starting point for the optimization of antimicrobial agents of potential clinical value in the fight against multiple-drug-resistant microorganisms.

KEYWORDS:

antibiotics · conformation analysis · drug design · NMR spectroscopy · peptidomimetics

Introduction

The growing problem of resistance to established antibiotics has stimulated intense interest in the development of novel antimicrobial agents with new modes of action. One emerging class of antibiotics is based on naturally occurring cationic peptides, which have been discovered in many animal species, where they are thought to constitute evolutionary ancient elements of innate immunity.[1, 2] These include disulfide-bridged β-hairpin and β-sheet peptides (for example, the protegrins,[3] tachyplesins,[4] and defensins[5]), amphipathic α-helical peptides (for example, cecropins, dermaseptins, magainins, and mellitins),[6] as well as other linear and loop-structured peptides.[7] The primary site of interaction of these cationic peptides is the microbial cell membrane.[2, 7] Upon exposure to these agents, the cell membrane undergoes permeabilization, which leads to rapid cell death.

Structural studies by NMR spectroscopy have shown that protegrin I[8, 9] and tachyplesin I[10] adopt well-defined β-hairpin conformations in water, as a result of the constraining effect of two disulfide bridges (Scheme 1). In protegrin analogues that lack one or both of the disulfide bonds, the stability of the β-hairpin conformation is diminished and the membranolytic activity is reduced.[11–14] Similar observations have been made in analogues of tachyplesin I[15] and in hairpin-loop mimetics of rabbit defensin NP-2,[16] which indicates that the β-hairpin structure plays an important role in the activity of these molecules. In the case of the α-helical cationic peptides, the amphiphilic nature of the helix appears to be important for their antimicrobial activity.[6]

A novel cyclic antimicrobial peptide RTD-1 was isolated recently from primate leukocytes.[17] This peptide contains three disulfide bridges, which act to constrain the cyclic peptide backbone into a hairpin geometry (Scheme 1).[18] Protegrin and tachyplesin analogues that contain a cyclic peptide backbone as well as multiple disulfide bridges to enforce an amphiphilic hairpin structure, have also been studied.[19–21]

[a] *Prof. J. A. Robinson, Dr. S. C. Shankaramma, Z. Athanassiou, Dr. K. Moehle, Dr. J. W. Vrijbloed*
Institute of Organic Chemistry
University of Zürich
Winterthurerstrasse 190, 8057 Zürich (Switzerland)
Fax: (+41) 1635-6833
E-mail: robinson@oci.unizh.ch

[b] *Dr. O. Zerbe*
Institute of Pharmaceutical Sciences
ETH-Zürich, Winterthurerstrasse 190
8057 Zürich (Switzerland)

[c] *Dr. C. Mouton, Dr. F. Bernardini, Dr. D. Obrecht*
Polyphor AG, Gewerbestrasse 14
4123 Allschwil (Switzerland)

Supporting information for this article is available on the WWW under http://www.chembiochem.org or from the author.

  1439-4227/02/03/11 $ 20.00+.50/0 ChemBioChem **2002**, 3, 1126 – 1133

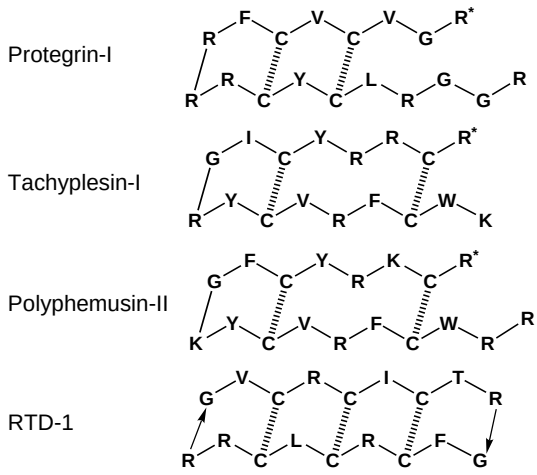

Scheme 1. *Naturally occurring β-hairpin antimicrobial peptides. R* = C-terminal arginine amide; C|||C = disulfide bridge.*

Other novel classes of cationic peptides have been reported, including those based on the cyclic D,L-α-peptide architecture[22] and on β-peptide scaffolds.[23–25] Mention should also be made of the cationic sulfur-bridged lantibiotics.[26]

A key issue in the design of new cationic antimicrobial peptides is selectivity. The naturally occurring protegrins and tachyplesins exert a significant hemolytic activity against human red blood cells, a key indicator of toxicity. This is also the case for protegrin analogues such as IB367,[12] a molecule now undergoing clinical trials for the treatment and prevention of oral mucositis. This high hemolytic activity represents a serious disadvantage for in vivo applications.

We describe below an approach to the synthesis of new antimicrobial peptidomimetics, based on the natural products protegrin, polyphemusin, and tachyplesin (Scheme 1). This method involves grafting the cationic hairpin sequence onto an organic template whose function is to restrain the peptide loop termini in a β-hairpin geometry. The concept of template-bound β-hairpin mimetics has been presented already,[27, 28] but such molecules have not previously been evaluated as antimicrobial agents. Here, we show that potent and selective antimicrobial β-hairpin mimetics are achievable and provide data on their conformation in water and in a membrane-mimetic environment. The ability to generate such peptidomimetics by using combinatorial and parallel synthesis methods[29] may greatly aid structure – activity studies on this interesting new class of molecules.

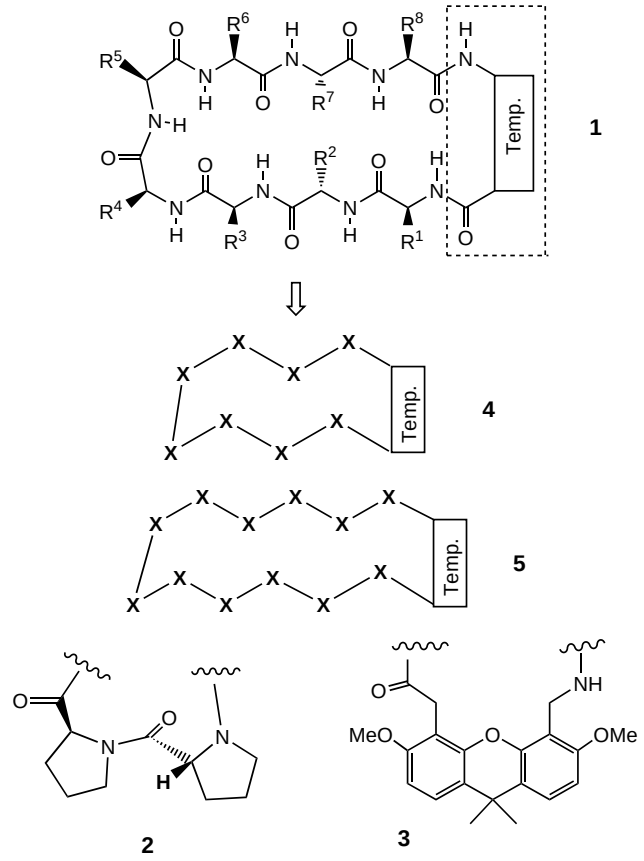

Scheme 2. *β-Hairpin mimetics studied in this work. X = cationic and/or hydrophobic/aromatic amino acid residues, Temp. = template **2** or **3**.*

We therefore set out to prepare libraries of cationic hairpin mimetics of the general types **4** and **5**, which contain eight or twelve residues, where X represents the cationic and hydrophobic/aromatic amino acids typically found in the natural products shown in Scheme 1.

A two-stage synthetic strategy was followed,[29] in which a linear precursor was first assembled on chlorotrityl-polystyrene resin by using 9-fluorenylmethoxycarbonyl (Fmoc) solid-phase peptide chemistry (Scheme 3).[32] After release from the resin, the fully-assembled linear precursors were cyclized in solution. In the final step, all side-chain protecting groups were removed upon treatment with trifluoroacetic acid. The desired mimetics were the main component (typically 50 – 80%) in the crude products, and were purified by HPLC, characterized by mass spectrometry, and then assayed for antimicrobial activity.

Results

Design and synthesis of mimetics

It has been shown previously that both 8- (for example, **1**) and 12-residue loops attached to a D-Pro-L-Pro template (**2**) can adopt regular β-hairpin conformations (such as that depicted by **1**; Scheme 2),[29, 30] and similar conformations have been observed in loops of various sizes attached to the xanthene template **3**.[31]

Antimicrobial activity

Screening of a library of 12-residue mimetics of type **5**, which contain templates **2** or **3**, gave several members with activity against Gram-positive and Gram-negative bacteria, as well as the yeast *Candida albicans* (Table 1). No mimetics with comparable activity were found in a small library of 8-residue mimetics of type **4** (data not shown). Within the family of 12-residue mimetics **5**, significant differences in selectivity were observed

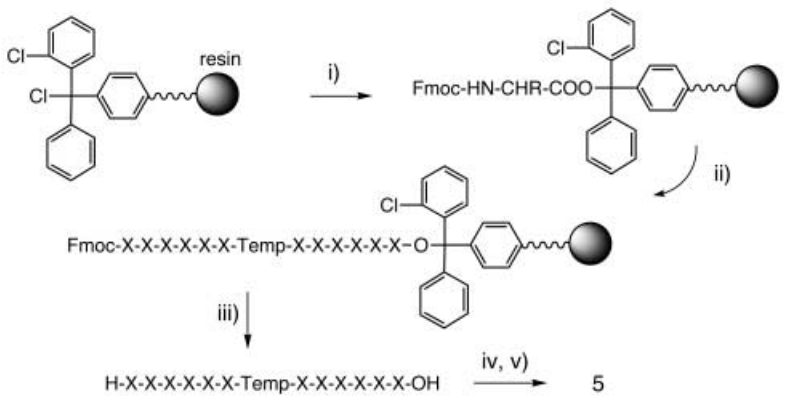

Scheme 3. *Reagents: i) Fmoc amino acid residue, iPr_2NEt, CH_2Cl_2; ii) cycles of peptide assembly with 20% piperidine in NMP for Fmoc removal and HOBt/HBTU for coupling; iii) 20% piperidine in NMP, then 1% CF_3COOH in CH_2Cl_2; iv) iPr_2NEt, HOAt, HATU; v) CF_3COOH, thioanisole, phenol, H_2O, $HSCH_2CH_2SH$, iPr_3SiH (82.5:5:5:2.5:2.5:2.5). X = (S)-α-amino acid residue; Temp = template **2** or **3**.*

between microbial cells and human red blood cells. Mimetic 4 is of special interest (Table 1) and has a good antimicrobial spectrum and a low hemolytic activity.

Kinetic studies reveal that bacterial cells are killed rapidly upon exposure to mimetic 4 at the MIC. Microscopic examination of the cell debris indicated rupture of the cell membrane, as for cells treated with protegrin I. At the MIC, the number of viable bacterial cells is reduced within minutes by three orders of magnitude, which indicates that mimetic 4 has a strong bactericidal activity (data not shown).

To examine the effect of the mimetic on membrane potential, *Staphylococcus aureus* cells were saturated with the potential-sensitive dye 3,3′-dihexyloxacarbocyanine iodide [$diSC_3(5)$].[33, 34] Upon treatment of these cells with mimetic 4 at the MIC, a large increase in fluorescence was observed, consistent with almost complete membrane depolarization (Figure 1).

Two mimetics were prepared containing a disulfide bridge (mimetics 6 and 7) as an additional conformational constraint. These are analogues of mimetic 4, but both displayed a reduced antimicrobial activity (Table 1).

Conformation studies

The conformation of mimetic 4 was studied by ^{1}H NMR spectroscopy, both in water at pH 2.3 and when bound to dodecylphosphocholine (DPC) micelles as a membrane-mimetic environment. The ^{1}H NMR spectrum in water revealed three molecular species, in a ratio of approximately 5:15:80, that do not interconvert on the NMR timescale. A chirality analysis after total acid hydrolysis indicated that the minor species were not the result of epimerization during synthesis. At least one of the minor forms may arise as a result of *cis*/*trans* isomerism at the Val-D-Pro peptide bond; this conclusion is consistent with the frequent observation of an increased proportion of *cis* conformer at Xaa – Pro peptide bonds (where Xaa = an amino acid). Severe signal overlap prevented resonance assignments of the minor components, and hence only the major species was considered for further analysis. The ^{1}H NMR spectra of the major form in water and in micelles were assigned (see the Supporting Information) by using 2D DQF-COSY, TOCSY and ROESY, or NOESY spectra, following established methods.[35]

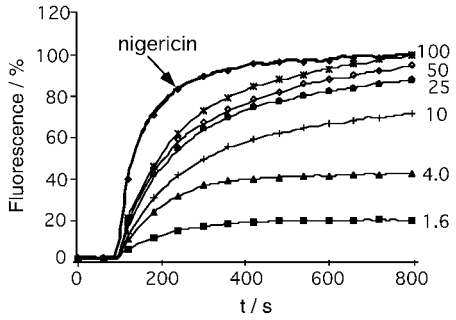

Figure 1. *Fluorescence changes (λ_{ex} = 622 nm, λ_{em} = 660 nm) of $diSC_3(5)$ in the presence of* S. aureus *cells, caused by addition of mimetic 4 (1.6, 4, 10, 25, 50, and 100 μg mL^{-1}) or nigericin (100 μg mL^{-1}). The rates of membrane depolarization correlate with the change in fluorescence intensity, which is assumed to be 100% with nigericin.*

Table 1. *Assays of antibiotic and hemolytic activity.*

Mimetic	Sequence-template (**2** or **3**)[a]	MIC[b] [μg mL^{-1}]				% Hemolysis[c] (at 100 μg mL^{-1})
		S. aureus	*E. coli*	*P. aerug*	*C. albic*	
mimetic 1	LRLKYRRFKYRV-**2**	25	12	25	12	27
mimetic 2	LRLQYRRFQYRV-**2**	12	6	12	6	27
mimetic 3	LRLEYRRFEYRV-**2**	100	100	> 100	50	14
mimetic 4	LRLKKRRWKYRV-**2**	12	12	6	12	1
mimetic 5	LRLKKRRWKYRV-**3**	6	25	25	6	13
mimetic 6	LCLKKRRWKYCV-**2**	25	6	25	12	3
mimetic 7	LRCKKRRWKCRV-**2**	25	25	50	50	1
	Protegrin I	6	3	3	6	37
	Tachyplesin I	2	1	2	2	34
	IB367	6	2	3	6	37

[a] Single-letter codes are used for the amino acid residues and sequences are given from the N to C terminus. The connectivity is shown in **5**. The template used (**2** or **3**) is also shown. The pair of cysteine residues in mimetic 6 and mimetic 7 each form a disulfide bond. [b] MIC = minimal inhibitory concentration in μg mL^{-1} of mimetic against *Staphylococcus aureus* ATCC 25923, *Escherichia coli* ATCC 25922, *Pseudomonas aeruginosa* ATCC 27853, and *Candida albicans*. The activities of protegrin I, tachyplesin I, and IB367 under these assay conditions are given for comparison as internal controls. [c] The hemolysis is the % hemolysis of fresh human red blood cells at a peptide concentration of 100 μg mL^{-1}.

The $^3J_{HN_\alpha}$ scalar coupling constants for mimetic 4 in water were mostly in the range 5 – 8 Hz; these values are indicative of rotationally-averaged ϕ backbone angles rather than regular β-hairpin structures. Moreover, very few cross-strand NOEs typical of regular β-hairpin structures were observed in NOESY spectra. Structure calculations were performed by simulated annealing (SA) by using NOE-derived upper distance restraints. Since very few long-range cross-strand NOEs were observed, it was not surprising that the resulting low-energy structures showed little convergence to a regular hairpin conformation (Figure 2).

Figure 2. *Average SA structures calculated for mimetic 4 in water at pH 2.3. The 13 low-energy structures were superimposed over the N, C(α), and C atoms of the* L-Pro-D-Pro *template.*

The $^3J_{HN_\alpha}$ values for mimetic 4 in the presence of perdeuterated DPC micelles were significantly larger than in water, with several residues adopting values in the range 8.5 – 9.0 Hz. In NOESY spectra, cross-strand NOEs characteristic of a β-hairpin were now present, including those between the amide protons of Leu1 and Val12, between Leu3 and Tyr10, and between Lys5 and Trp8 (see the Supporting Information). Furthermore, strong NOEs between the C(α)H protons in residues Arg2 and Arg11, as well as Lys4 and Lys9, were observed, which indicates a relatively stable β-hairpin structure. A superimposition of 18 low-energy DYANA structures (Figure 3) clearly revealed a regular hairpin-like fold. The root mean square deviation (RMSD) of the mean structure after superimposition of backbone and heavy atoms of all residues was 0.46 and 1.83 Å, respectively. Cross-strand hydrogen bonds were present in 15 of the 18 calculated structures between the Leu1 NH and Val12 CO groups and between the Val12 NH and Leu1 CO groups, and in most conformers also between the Leu3 NH and Tyr10 CO groups, as well as from the Tyr10 NH to the Leu3 CO group. All conformers contain a type-II′ β turn at the tip of the hairpin (residues Lys5 to Trp8), which is characterized by a Lys5—CO···Trp^8—NH hydrogen bond and a strong sequential NOE between the amide protons of Arg7 and Trp8.

Figure 3. *Average solution structures for mimetic 4 in the presence of DPC micelles. The 18 low-energy DYANA structures are superimposed over the backbone heavy atoms.*

Evidence for the association of mimetic 4 with DPC micelles was obtained from TOCSY spectra upon addition of the micelle-integrating spin labels 5-, 7-, or 12-doxylstearate. In the presence of 5- or 7-doxylstearate, the H^N,H^α cross peaks from residues Arg2, Lys4, and Arg11 were selectively attenuated by greater than 90% and that from Tyr10 to a somewhat lesser extent (> 70%; Figure 4). Protons in the D-Pro-L-Pro template were also affected to a large extent (> 80%) by 7-doxylstearate. In contrast, for both cases the reductions in cross-peak intensities from residues Lys5 to Trp8 were less than 50%. Only small effects were observed in samples that contained 12-doxylstearate. Further evidence for membrane association stems from changes in the chemical shifts, most probably induced by interactions of the mimetic with the polar head groups of the micelles.

Mimetics 6 and 7 were also studied in aqueous solution at pH 2.3 by NMR spectroscopy. The $^3J_{HN_\alpha}$ values and NOEs for mimetic 6 (data not shown) suggest that some degree of averaging occurs in aqueous solution. The ^{1}H NMR spectra of mimetic 7 in water has $^3J_{HN_\alpha}$ values for Leu1, Arg2, and Arg7 in the range 2 – 2.5 Hz, characteristic of a helical conformation, and for Arg6, Trp8, and Cys10 in the range 8.5 – 11 Hz, typical of β

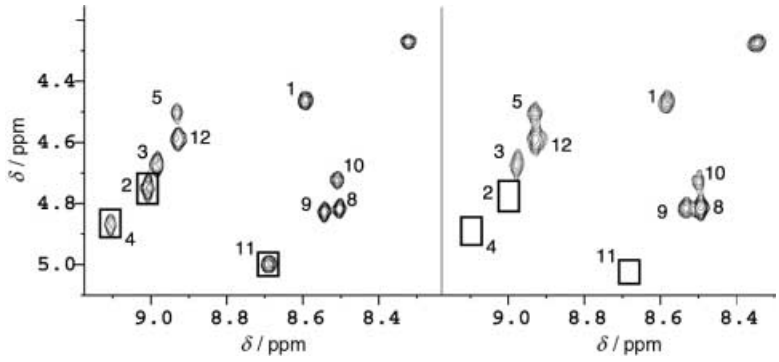

Figure 4. *Homonuclear [^{1}H,^{1}H]-TOCSY spectra of mimetic 4 in the presence of DPC micelles with (right) and without (left) the spin label 5-doxylstearic acid. The numbers refer to the residue numbers. The boxes highlight HN – HC(α) cross peaks that are strongly and selectively reduced in intensity in the presence of the spin label.*

structure. Several long-range cross-strand NOEs were observed (see the Supporting Information), as well as a strong NOE between the C(α)H atoms of Val12 and D-Pro13, which indicates a *cis*-Val^{12}-D-Pro^{13} peptide bond. The average solution structures calculated for mimetic 7 by using NOEs and well-defined angle constraints include a *cis*-Val12-D-Pro13 peptide bond and unexpectedly reveal a short stretch of 3_{10} helical conformation between residues 1 and 4 (Figure 5).

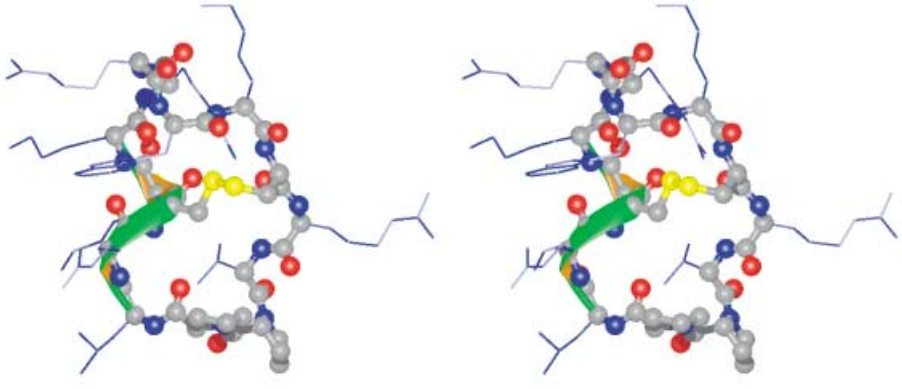

Figure 5. *Stereoview of one average solution structure deduced for mimetic 7 (O atoms = red, N atoms = blue, S atoms = yellow). The green ribbon represents the short region of 3_{10} helix.*

Discussion

The design of the mimetics reported here starts from the premise that a suitably chosen template will stabilize a regular 2:2 or 2:4 β-hairpin conformation[36] in either 8- or 12-residue loops (**4** or **5**, respectively). In practice, no 8-residue mimetics of type **4** were found to have significant antimicrobial activity, so attention focused on the 12-residue mimetics **5**. The topology of a regular 12-residue hairpin is depicted schematically in **6**, which conveniently illustrates the clustering of side-chains in residues 1, 3, 5, 8, 10, and 12 on one face of the hairpin, and residues 2, 4, 9, and 11 on the other.

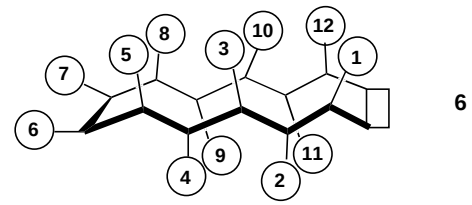

6

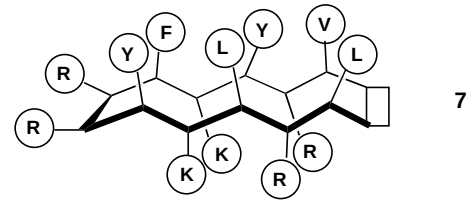

7

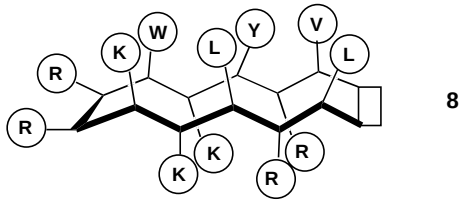

8

The 12-residue mimetic 1 (Table 1) has significant antimicrobial activity against Gram-positive and Gram-negative bacteria as well as *C. albicans*. This mimetic has an apparent amphipathic nature, with six hydrophobic/aromatic groups clustering on the upper face and four positively charged groups on the lower face of a regular hairpin structure as shown in **7**. However, mimetic 1 also shows a significant hemolytic activity against human red blood cells. The hemolytic activity is lower, however, than that found here for the natural product protegrin I (Table 1). Mimetic 2 has two fewer cationic groups and also possesses good antimicrobial activity, but the hemolytic activity remains high, whereas the introduction of glutamic acid (mimetic 3) leads to a loss of antimicrobial activity (Table 1).

An important observation is that breaking the apparent amphipathic nature of the hairpin by introducing a cationic residue onto the upper face, as in mimetic 4 (**8**), leads to a large improvement in selectivity, as evidenced by the somewhat higher antimicrobial activity and much lower hemolytic activity (Table 1). It is of interest that the xanthene template **3** in mimetic 5, gives a higher selectivity towards the Gram-positive microorganism *S. aureus*, but at the cost of a somewhat higher hemolytic activity (Table 1). These results show that it is possible to separate the antimicrobial and hemolytic activities in this class of mimetics and influence whether they target Gram-positive or Gram-negative bacteria by variations in the hairpin sequence as well as in the template.

To develop structure – activity studies, it was important to characterize the preferred conformations of mimetic 4 in aqueous solution and in a membrane-mimetic environment. The NMR properties of mimetic 4 ($^3J_{HN_\alpha}$ values in the range 6 – 8 Hz, with few cross-strand NOEs) strongly suggest that this molecule is largely unstructured in water, despite the influence of the D-Pro-L-Pro template (see Figure 2). In the presence of DPC micelles, on the other hand, mimetic 4 clearly adopts a regular β-hairpin conformation ($^3J_{HN_\alpha}$ values greater than 8.5 Hz, with many characteristic cross-strand NOEs) (Figure 3). DPC micelles have frequently been used as a membrane-mimetic environment in NMR studies of membrane-active peptides and proteins.[37] It is possible that mimetic 4 will undergo a similar conformational transition to a well-defined hairpin structure upon interaction with the lipid bilayer of a cell membrane. However, more detailed biophysical studies are needed to confirm this conclusion.

The naturally occurring cationic hairpin peptides protegrin[8, 9] and tachyplesin,[10, 38] adopt well-defined β-hairpin structures in aqueous solution. The behavior of mimetic 4, however, parallels that of some linear cationic peptides that adopt amphipathic α helices only upon interaction with a membrane-like environment.[2] Other studies have suggested that protegrin I may form dimeric structures when bound to DPC micelles,[39] although no evidence for di- or oligomerization of mimetic 4 was found in this work.

A somewhat decreased antimicrobial activity was observed for mimetics 6 and 7, each of which contains a disulfide bridge. We envisaged that the disulfide bridge would help to stabilize a regular hairpin structure. However, NMR studies showed that mimetic 7 possesses a well-defined but unusual loop structure

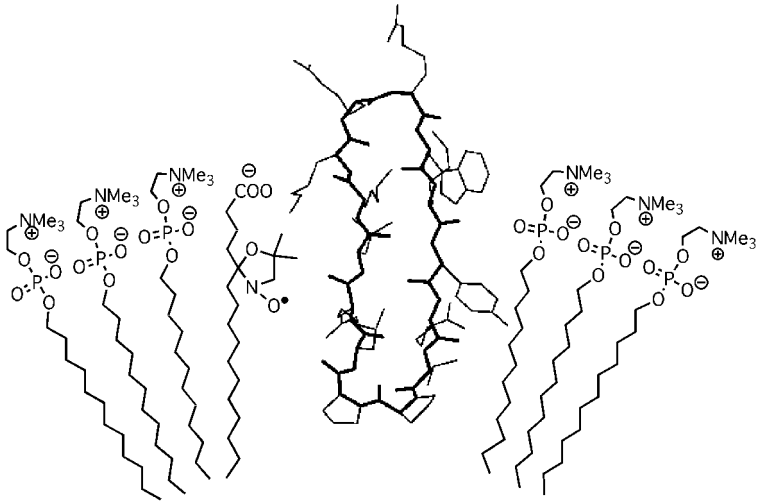

Figure 6. *A representation of mimetic 4 in DPC micelles together with 5-doxylstearate (see the Discussion for an explanation).*

with a *cis*-Val12-D-Pro13 peptide bond (Figure 5). A regular β-hairpin geometry is clearly not present in mimetic 7, although a short stretch of 3_{10} helix is seen. This unexpected result illustrates the importance of structural studies to establish empirically deduced conformations in peptidomimetics.

To demonstrate the interaction of mimetic 4 with the micelle surface, NMR experiments were also performed in the presence of 5-, 7-, or 12-doxylstearate. These lipids contain a stable cyclic nitroxide free radical (see Figure 6), whose unpaired electron leads to accelerated longitudinal and transverse relaxation for protons in close spatial proximity. The label in 12-doxylstearate is located near to the center of the hydrophobic micelle core, whereas that in the 5-doxylstearate is closer to the polar head groups near the surface of the micelle. Addition of 5- or 7-doxylstearate selectively attenuated TOCSY cross peaks for residues Arg2, Lys4, Tyr10, and Arg11 (Figure 4), and protons in the D-Pro-L-Pro template were additionally affected to a large extent by 7-doxylstearate. It follows, therefore, that mimetic 4 inserts at least partially into the micelle under these conditions, with the template positioned in the hydrophobic interior and the largely cationic tip of the hairpin (Lys5, Arg6, Arg7, and Phe8) possibly close to or extended into the aqueous phase (Figure 6). Although the data do not allow a precise description of the orientation(s) of the mimetic in the micelle, the results are not consistent with the hairpin lying parallel along the surface of the micelle, at least at the concentrations used in this NMR study.

Two distinct membrane-bound states have been detected with protegrin I.[40, 41] The S state has protegrin embedded in the head-group region and lying parallel to the plane of the lipid bilayer. At higher peptide concentrations a transition to the I state occurs in which the peptide now inserts into the membrane bilayer, which possibly leads to pore formation.

More detailed biophysical studies will be required to determine if a similar inserted orientation occurs upon binding of mimetic 4 to the bilayer of cell membranes and to determine the detailed mechanism of its antimicrobial action. The encouraging results obtained so far provide motivation to extend the structure – activity studies, an endeavor that may lead to new antibiotics of potential clinical value in combating multiple-drug-resistant microorganisms.

Experimental Section

Synthesis of mimetic 4: The synthesis of mimetic 4 is an example of a typical procedure. Fmoc-Arg(Pbf)-OH (1.2 equiv) was coupled to 2-chlorotrityl chloride resin (1.08 mmol g^{-1}) in the presence of diisopropylethylamine (4 equiv) in CH_2Cl_2. Following removal of the Fmoc group with 20% piperidine/*N*-methylpyrrolidone (NMP), chain elongation was performed sequentially with Fmoc-Lys-(Boc)-OH, Fmoc-Lys(Boc)-OH, Fmoc-Leu-OH, Fmoc-Arg(Pbf)-OH, Fmoc-Leu-OH, Fmoc-Pro-OH, Fmoc-D-Pro-OH, Fmoc-Val-OH, Fmoc-Arg(Pbf)-OH, Fmoc-Tyr(*t*Bu)-OH, Fmoc-Lys(Boc)-OH, Fmoc-Trp(Boc)-OH, and Fmoc-Arg(Pbf)-OH (each 4 equiv), by using 20% piperidine/NMP for Fmoc deprotection, 1-hydroxy-1*H*-benzotriazole/*O*-(benzotriazol-1-yl)*N*,*N*,*N*′,*N*′-tetramethyluronium hexafluorophosphate (HOBt/HBTU) for activation, diisopropylethylamine as a base and NMP as solvent. After completion of the synthesis, the linear peptide was cleaved from the resin with 1% CF_3COOH in CH_2Cl_2. The product was then cyclized overnight at RT in 1% diisopropylethylamine/dimethylformamide with 7-aza-1-hydroxy-1*H*-benzotriazole (HOAt) and *N*-[(dimethylamino)-1*H*-1,2,3-triazole[4,5-*b*]-pyridin-1-ylmethylene]-*N*-methylmethanaminium hexafluorophosphate (HATU; 3 equiv). Deprotection with CF_3COOH, precipitation with diethyl ether, and purification by reversed phase HPLC (C18 column, gradient from 10 – 60% MeCN/H_2O + 0.1% CF_3COOH) gave mimetic 4. ESI-MS: *m*/*z*: 1879.9 $[M+H]^+$. See the Supporting Information for ^1H NMR assignments.

The mass spectral data for mimetics 1 to 7 are summarized in Table 2.

NMR studies: 1D ^1H and 2D NMR spectra of peptides in the absence of DPC were recorded in water at 600 MHz, 300 K (Bruker DRX-600 spectrometer), typically at a peptide concentration of approximately 7 – 8 mM, in H_2O/D_2O (9:1), and in D_2O, pH 2.3. The water signal was suppressed by presaturation. 2D spectra were analyzed by using Felix software (MSI, San Diego).

For structure calculations, NOEs were determined from ROESY or NOESY spectra measured with mixing times of 40, 80, 120, and 250 ms, with 1024 × 256 complex data points zero-filled prior to Fourier transformation to 2048 × 1024 data points and transformed with a cosine window function. Cross-peak volumes were determined by integration and build-up curves were checked to ensure a smooth exponential increase in peak intensity for NOEs used to

Table 2. *Observed m/z values for mimetics 1 to 7 measured by electrospray mass spectrometry.*

Mimetic	Calculated mass	Observed mass $[M+H]^+$; $[M+2H]^{2+}$
mimetic 1	1874.2	1875.0; 938.0
mimetic 2	1874.1	1875.0; 937.9
mimetic 3	1876.1	1877.1; 938.8
mimetic 4	1878.3	1879.9; 940.5
mimetic 5	2023.4	2024.4; 1012.7
mimetic 6	1770.2	1771.2
mimetic 7	1806.2	1806.2; 904.1

derive distance restraints. Restrained molecular dynamics calculations following an SA protocol were performed by using the DISCOVER program (MSI, San Diego) and molecular dynamics simulations with time-averaged distance and angle restraints were performed with the GROMOS96 software[42] by using methods described in detail earlier.[30]

NMR studies in the presence of micelles were conducted on a sample of mimetic 4 (2 mM) at 310 K, pH 5.0, in d_{38}-DPC (300 mM) in 90% H_2O/10% H_2O or 99.9% D_2O. Spin labels were added at a concentration of about 5 mM to yield about one spin label per micelle. Amino acid spin systems of mimetic 4/DPC were identified from a 12-ms clean TOCSY[43] experiment. NOESY experiments (75 ms)[44, 45] incorporating a filter scheme for zero-quantum suppression[46] were used for both the sequence-specific sequential resonance assignment and the determination of upper proton–proton distance limits required for structure calculations. Water suppression was achieved by using the WATERGATE sequence.[47] Scalar $^3J_{HN_\alpha}$ coupling constants were derived from inverse Fourier transformation of in-phase NOESY peaks that involved H^N protons.[48] The structure calculation was performed by restrained molecular dynamics in torsion angle space by applying the SA protocol implemented in the program DYANA.[49] Restrained energy minimization was performed with the OPAL software,[50] which utilizes the AMBER force-field. RMSD values were calculated with the program MOLMOL,[51] which was also used to prepare Figures 3 and 5.

Antimicrobial assays: The antimicrobial activities were determined by the standard National Committee for Clinical Laboratory Standards broth microdilution method. Innocula of the microorganisms were diluted into Mueller–Hinton (MH) broth to give approximately 10^6 colony forming units (CFU) per mL for bacteria or 5×10^3 CFU mL^{-1} for *Candida*. Aliquots (50 µL) of the innocula were added to MH broth (50 µL) containing the peptide in serial two-fold dilutions. Antimicrobial activities are expressed as the minimal inhibitory concentration in µg mL^{-1}, the concentration at which 100% inhibition of growth was observed after 18–20 h incubation at 37 °C. Determinations were performed in triplicate.

Hemolytic activity: Fresh human red blood cells were washed three times with phosphate-buffered saline (PBS), and then incubated with peptide at a concentration of 100 µg mL^{-1} for 1 h at 37 °C. The final erythrocyte concentration was approximately 0.9×10^9 mL^{-1}. The values at 0% and 100% lyses were determined by incubation of cells with PBS or 0.1% Triton X-100 in water, respectively. The samples were centrifuged, the supernatant diluted twentyfold in PBS, and the optical density was measured at 540 nm.

Cell depolarization assay: Logarithmic-growth *S. aureus* (ATCC 25923) cells were harvested by centrifugation (1500 × g) and washed once with buffer (HEPES (5 mM), pH 7.3) that contained glucose (20 mM). The cells were resuspended to an optical density of 0.05 at 600 nm in a buffer (HEPES (5 mM), pH 7.3 and KCl (0.1 M)) that contained glucose (20mM) and stained for 30 min at room temperature in the dark with 3,3′-dihexyloxacarbocyanine iodide [diSC_3(5)] (1 µM). Fluorescence readings were carried out in a Luminescence Spectrometer (Perkin–Elmer). Nigericin (100 µg mL^{-1}) and peptide mimetic 4 (6 µg mL^{-1}) were added to the cuvette at $t = 100$ s and the fluorescence ($\lambda_{ex} = 622$ nm, $\lambda_{em} = 660$ nm) was monitored over an additional 700 s (Figure 1).

The authors are grateful to the Swiss National Science Foundation and the Swiss Commission for Technology and Innovation for supporting this work, and to Annelies Meier for expert technical assistance.

[1] M. G. Scott, R. E. W. Hancock, *Crit. Rev. Immunol.* **2000**, *20*, 407.
[2] W. vantHof, E. C. I. Veerman, E. J. Helmerhorst, A. V. N. Amerongen, *Biol. Chem.* **2001**, *382*, 597.
[3] V. N. Kokryakov, S. S. L. Harwig, E. A. Panyutich, A. A. Shevchenko, G. M. Aleshina, O. V. Shamova, H. A. Korneva, R. I. Lehrer, *FEBS Lett.* **1993**, *327*, 231.
[4] T. Nakamura, H. Furunaka, T. Miyata, F. Tokunaga, T. Muta, S. Iwanaga, M. Niwa, T. Takao, Y. Shimonishi, *J. Biol. Chem.* **1988**, *263*, 16709.
[5] R. I. Lehrer, A. K. Lichtenstein, T. Ganz, *Annu. Rev. Immunol.* **1993**, *11*, 105.
[6] A. Tossi, L. Sandri, A. Giangaspero, *Biopolymers* **2000**, *55*, 4.
[7] R. N. McElhaney, E. J. Prenner, *Biochim. Biophys. Acta* **1999**, *1462*, 1.
[8] R. L. Fahrner, T. Dieckmann, S. S. L. Harwig, R. I. Lehrer, D. Eisenberg, J. Feigon, *Chem. Biol.* **1996**, *3*, 543.
[9] A. Aumelas, M. Mangoni, C. Roumestand, L. Chiche, E. Despaux, G. Grassy, B. Calas, A. Chavanieu, *Eur. J. Biochem.* **1996**, *237*, 575.
[10] K. Kawano, T. Yoneya, T. Miyata, K. Yoshikawa, F. Tokunaga, Y. Terada, S. Iwanaga, *J. Biol. Chem.* **1990**, *265*, 15365.
[11] H. Tamamura, T. Murakami, S. Noriuchi, K. Sugihara, A. Otaka, W. Takada, T. Ibuka, M. Waki, N. Tamamoto, N. Fujii, *Chem. Pharm. Bull.* **1995**, *43*, 853.
[12] J. Chen, T. J. Falla, H. J. Liu, M. A. Hurst, C. A. Fujii, D. A. Mosca, J. R. Embree, D. J. Loury, P. A. Radel, C. C. Chang, L. Gu, J. C. Fiddes, *Biopolymers* **2000**, *55*, 88.
[13] S. L. Harwig, A. Waring, H. J. Yang, Y. Cho, L. Tan, R. J. Lehrer, *Eur. J. Biochem.* **1996**, *240*, 352.
[14] M. E. Mangoni, A. Aumelas, P. Charnet, C. Roumestand, L. Chiche, E. Despaux, G. Grassy, B. Calas, A. Chavanieu, *FEBS Lett.* **1996**, *383*, 93.
[15] H. Tamamura, R. Ikoma, M. Niwa, S. Funakoshi, T. Murakami, N. Fujii, *Chem. Pharm. Bull.* **1993**, *41*, 978.
[16] S. Thennarasu, R. Nagaraj, *Biochem. Biophys. Res. Commun.* **1999**, *254*, 281.
[17] Y.-Q. Tang, J. Yuan, G. Ösapay, K. Ösapay, D. Tran, C. J. Miller, A. J. Oellette, M. E. Selsted, *Science* **1999**, *286*, 498.
[18] M. Trabi, H. J. Schirra, D. J. Craik, *Biochemistry* **2001**, *40*, 4211.
[19] J. P. Tam, C. Wu, J.-L. Yang, *Eur. J. Biochem.* **2000**, *267*, 3289.
[20] J. P. Tam, Y.-A. Lu, J.-L. Yang, *Biochemistry* **2000**, *39*, 7159.
[21] J. P. Tam, Y.-A. Lu, J.-L. Yang, *Biochem. Biophys. Res. Comm.* **2000**, *267*, 783.
[22] S. FernandezLopez, H. S. Kim, E. C. Choi, M. Delgado, J. R. Granja, A. Khasanov, K. Kraehenbuehl, G. Long, D. A. Weinberger, K. M. Wilcoxen, M. R. Ghadiri, *Nature* **2001**, *412*, 452.
[23] D. H. Liu, W. F. DeGrado, *J. Am. Chem. Soc.* **2001**, *123*, 7553.
[24] E. A. Porter, X. F. Wang, H. S. Lee, B. Weisblum, S. H. Gellman, *Nature* **2000**, *404*, 565.
[25] P. I. Arvidsson, J. Frackenpohl, N. S. Ryder, B. Liechty, F. Petersen, H. Zimmermann, G. P. Camenisch, R. Woessner, D. Seebach, *ChemBioChem* **2001**, *2*, 771.
[26] R. W. Jack, G. Jung, *Curr. Opin. Chem. Biol.* **2001**, *4*, 310.
[27] J. A. Robinson, *Syn. Lett.* **2000**, *4*, 429.
[28] D. Obrecht, M. Altorfer, J. A. Robinson, *Adv. Med. Chem.* **1999**, *4*, 1.
[29] L. Jiang, K. Moehle, B. Dhanapal, D. Obrecht, J. A. Robinson, *Helv. Chim. Acta* **2000**, *83*, 3097.
[30] M. Favre, K. Moehle, L. Jiang, B. Pfeiffer, J. A. Robinson, *J. Am. Chem. Soc.* **1999**, *121*, 2679.
[31] K. Müller, D. Obrecht, A. Knierzinger, C. Stankovic, C. Spiegler, W. Bannwarth, A. Trzeciak, G. Ebglert, A. M. Labhardt, P. Schönholzer in *Building Blocks for the Induction or Fixation of Peptide Conformations*, (Eds.: B. Testa, E. Kyburz, W. Fuhrer, R. Giger), Verlag Helvetica Chimica Acta, Basel, **1993**, p. 513.
[32] W. C. Chan, P. D. White in *Fmoc Solid Phase Peptide Synthesis: A Practical Approach*, (Ed.: B. D. Hames), Oxford University Press, Oxford, **2000**.
[33] A. S. Waggoner, *Annu. Rev. Biophys. Bioeng.* **1979**, *8*, 47.
[34] L. M. Loew, *Adv. Chem. Ser.* **1994**, *235*, 151.
[35] K. Wüthrich, *NMR or Proteins and Nucleic Acids*, Wiley Interscience, **1986**.
[36] B. L. Sibanda, T. L. Blundell, J. M. Thornton, *J. Mol. Biol.* **1989**, *206*, 759.
[37] G. D. Henry, B. D. Sykes, *Methods Enzymol.* **1994**, *239*, 515.
[38] H. Tamamura, M. Kuroda, M. Masada, A. Otaka, S. Funakoshi, H. Nakashima, N. Yamamoto, M. Waki, A. Matsumoto, J. M. Lancelin, D. Kohda, S. Tate, F. Inagaki, N. Fujii, *Biochim. Biophys. Acta* **1993**, *1163*, 209.
[39] C. Roumestand, V. Louis, A. Aumelas, G. Grassy, B. Calas, A. Chavanieu, *FEBS Lett.* **1998**, *421*, 263.
[40] W. T. Heller, A. J. Waring, R. I. Lehrer, H. W. Huang, *Biochemistry* **1998**, *37*, 17331.

[41] W. T. Heller, A. J. Waring, R. I. Lehrer, T. A. Harroun, T. M. Weiss, L. Yang, H. W. Huang, *Biochemistry* **2000**, *39*, 139.
[42] W. F. van Gunsteren, S. R. Billeter, A. A. Eising, P. H. Hünenberger, P. Krüger, A. E. Mark, W. R. P. Scott, I. G. Tironi, *Biomolecular Simulation: The GROMOS96 Manual and User Guide*, Hochschulverlag AG an der ETH Zürich, **1996**.
[43] C. Griesinger, G. Otting, K. Wüthrich, R. R. Ernst, *J. Am. Chem. Soc.* **1988**, *110*, 7870.
[44] A. Kumar, R. R. Ernst, K. Wüthrich, *Biochem. Biophys. Res. Comm.* **1980**, *95*, 1.
[45] S. Macura, R. R. Ernst, *Mol. Phys.* **1980**, *41*, 95 – 117.
[46] G. Otting, *J. Magn. Reson.* **1990**, *86*, 496.
[47] M. Piotto, V. Saudek, V. Sklenar, *J. Biomol. NMR* **1992**, *2*, 661.
[48] T. Szyperski, P. Güntert, G. Otting, K. Wüthrich, *J. Magn. Reson.* **1992**, *99*, 552.
[49] P. Güntert, C. Mumenthaler, K. Wüthrich, *J. Mol. Biol.* **1997**, *273*, 283.
[50] P. Luginbühl, P. Güntert, M. Billeter, K. Wüthrich, *J. Biomol. NMR* **1997**, *9*, 212.
[51] R. Koradi, M. Billeter, K. Wüthrich, *J. Mol. Graphics* **1996**, *14*, 51.

Received: February 22, 2002 [F368]
Publication delayed at author's request.